AD/A-003 246

THE EFFECT OF ANGULAR VELOCITY AND COMPOSITION ON PYROTECHNIC PERFORMANCE

Walter J. Puchalski

Frankford Arsenal
Philadelphia, Pennsylvania

August 1974

DISTRIBUTED BY:

NTIS
National Technical Information Service
U. S. DEPARTMENT OF COMMERCE

UNCLASSIFIED

SECURITY CLASSIFICATION OF THIS PAGE (When Data Entered)

REPORT DOCUMENTATION PAGE		READ INSTRUCTIONS BEFORE COMPLETING FORM
1. REPORT NUMBER FA-TR-74011	2. GOVT ACCESSION NO.	3. RECIPIENT'S CATALOG NUMBER AD/A-003246
4. TITLE (and Subtitle) THE EFFECT OF ANGULAR VELOCITY AND COMPOSITION ON PYROTECHNIC PERFORMANCE		5. TYPE OF REPORT & PERIOD COVERED Technical research report 6. PERFORMING ORG. REPORT NUMBER
7. AUTHOR(s) WALTER J. PUCHALSKI		8. CONTRACT OR GRANT NUMBER(s)
9. PERFORMING ORGANIZATION NAME AND ADDRESS Frankford Arsenal Attn: SARFA-MDP-Y Philadelphia, PA 19137		10. PROGRAM ELEMENT, PROJECT, TASK AREA & WORK UNIT NUMBERS AMCMS CODE: 662603.11.H7800 DA PROJ: 1W662603AH78
11. CONTROLLING OFFICE NAME AND ADDRESS ARMCOM		12. REPORT DATE August 1974 13. NUMBER OF PAGES 37
14. MONITORING AGENCY NAME & ADDRESS (if different from Controlling Office)		15. SECURITY CLASS. (of this report) UNCLASSIFIED 15a. DECLASSIFICATION/DOWNGRADING SCHEDULE N/A

16. DISTRIBUTION STATEMENT (of this Report)

Approved for public release; distribution unlimited.

17. DISTRIBUTION STATEMENT (of the abstract entered in Block 20, if different from Report)

18. SUPPLEMENTARY NOTES

19. KEY WORDS (Continue on reverse side if necessary and identify by block number)

Pyrotechnics	Burning Rate
Tracers	Slag Percent
Magnesium	Luminosity
Strontium Nitrate	Burning Rate Equation
Spin	

20. ABSTRACT (Continue on reverse side if necessary and identify by block number)

The influence of angular velocity on the light output, slag retention, and burning rate of magnesium/strontium nitrate pyrotechnic compositions consolidated into metal cavities is discussed. Stoichiometric, as well as, non-stoichiometric fuel/oxidizer mixtures were studied at rotational speeds up to 43,000 rpm and a parametric burning-rate equation was developed. In addition, qualitative descriptions of the burning phenomena and its effects are presented.

DD FORM 1 JAN 73 1473 EDITION OF 1 NOV 65 IS OBSOLETE

UNCLASSIFIED

SECURITY CLASSIFICATION OF THIS PAGE (When Data Entered)

TABLE OF CONTENTS

List of Illustrations

List of Tables

INTRODUCTION

Previous investigations on the effects of spin rate and cavity geometry on burn time and candlepower output[1, 2] had the objective of correlating laboratory performance with field performance. When standard tracer and igniter compositions were used in tracer cavities, results of laboratory testing indicated a linear relationship between burning time and projectile spin rate for lower spin rates and an asymptotic value of burning time at higher spin rates. No correlations between burning rate and compositions were reported.

When dealing with a standard tracer mixture, not only is the investigator examining the fuel and oxidizer, but also any binder, burning rate modifier, and/or color agent(s) which were added to meet a specific requirement. The other ingredients comprising these mixtures tend to mask the roles of the fuel and the oxidizer. In this work all components, except the fuel and the oxidizer, have been removed in order to examine their effects in a pyrotechnic reaction.

In the present work, cavities containing binary (fuel/oxidizer) pyrotechnic mixtures were evaluated relative to their output characteristics, with the independent variables being fuel/oxidizer ratio and cavity spin rate, and the dependent variables being average linear burning rate, candlepower, and percent slag retained in the column after burning.

EXPERIMENTATION

The experimental arrangement for this investigation is presented schematically in Figure 1. The major components consisted of a spinner (to hold both the sample and impart spin); a photocell (to detect and convert light output to measurable electrical signals); and an oscilloscope (to display the output). Auxiliary equipment included a

---

[1] R. Shulman, "Factors Affecting Small Arms Tracer Burning", Frankford Arsenal Technical Report R-1287 (September 1955).

[2] R. Shulman, "Effect of Cavity Geometry Upon Small Arms Tracer Burning", Frankford Arsenal Technical Report R-1421 (November 1957).

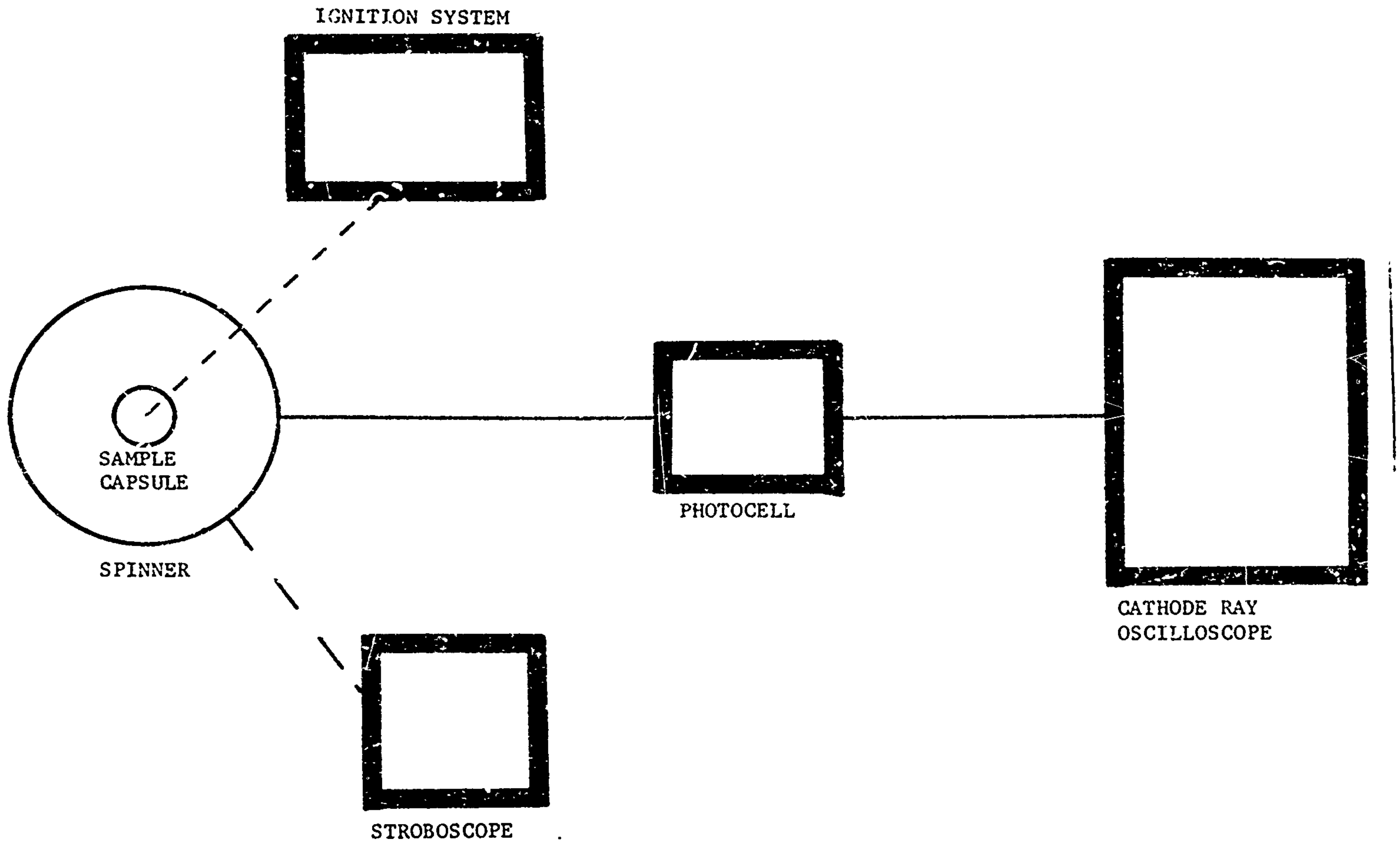

Figure 1. Pyrotechnic Performance Test Apparatus

photometer, a pyrotechnic ignition system, a stroboscope, and an oscilloscope recording camera.

The air-driven spinner (Figure 2), patterned after spinners described by Beams and Pickels[3], is presented in an exploded view in Figure 3. The spinner is operated by passing air through the inlet port and the holes in the stator. Air jets from the stator provide an air cushion between the stator and the rotor, and strike the flutes along the conical portion of the rotor, causing rotor spin. Air jet velocity (and consequently rotor rotational speed) is controlled by regulating the upstream air pressure.

Light from the burning sample was picked up by the photocell and transferred to the oscilloscope for photographic recording. Most tests were conducted with the photocell positioned three feet from the spinner; however, this distance was increased for higher candlepower values. To calibrate the vertical scale on the cathode ray tube (CRT), a 500 watt Mazda lamp was placed in the position of the spinner and a Weston Photometer was placed at the position of the photocell. The lamp voltage was controlled by a rheostat so that lamp output (in foot-candles) could be correlated with beam deflections in the vertical plane of the CRT.

The spin rates of the capsules were determined by placing an identifying mark on the rotor surface and noting (with a stroboscope) the fundamental speed at which the mark appeared stationary.

Ignition was accomplished by means of a spark from a Tesla coil. Each pyrotechnic sample, after being charged into its capsule, had pressed onto it a milligram quantity of a magnesium/barium peroxide (Mg/BaO_2) igniter mix and a spark-sensitive zirconium/lead dioxide (Zr/PbO_2) mix, respectively. After the sample was placed in the spinner and brought up to the desired spin rate, the Tesla coil was discharged igniting the Zr/PbO_2 mix and in turn igniting the sample.

The samples themselves were magnesium/strontium nitrate mixtures prepared by combining granulation 11 magnesium (MIL-M-382) with Grade B strontium nitrate (MIL-S-20322) after each was passed

[3] J. W. Beams, E. G. Pickels, "The Production of High Rotational Speeds", Rev. Sci. Inst. 6, (1935).

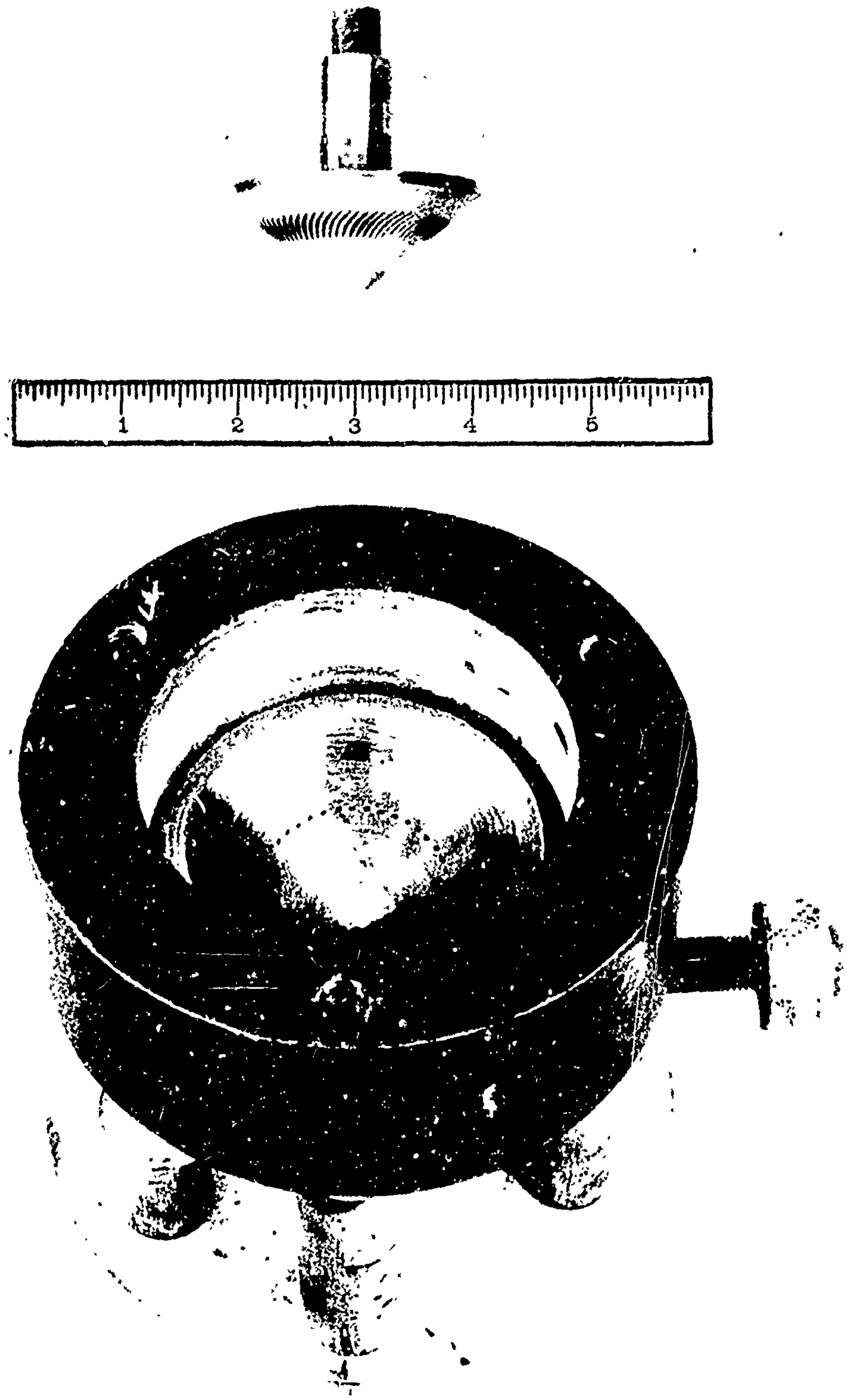

Figure 2. Bullet Spinner

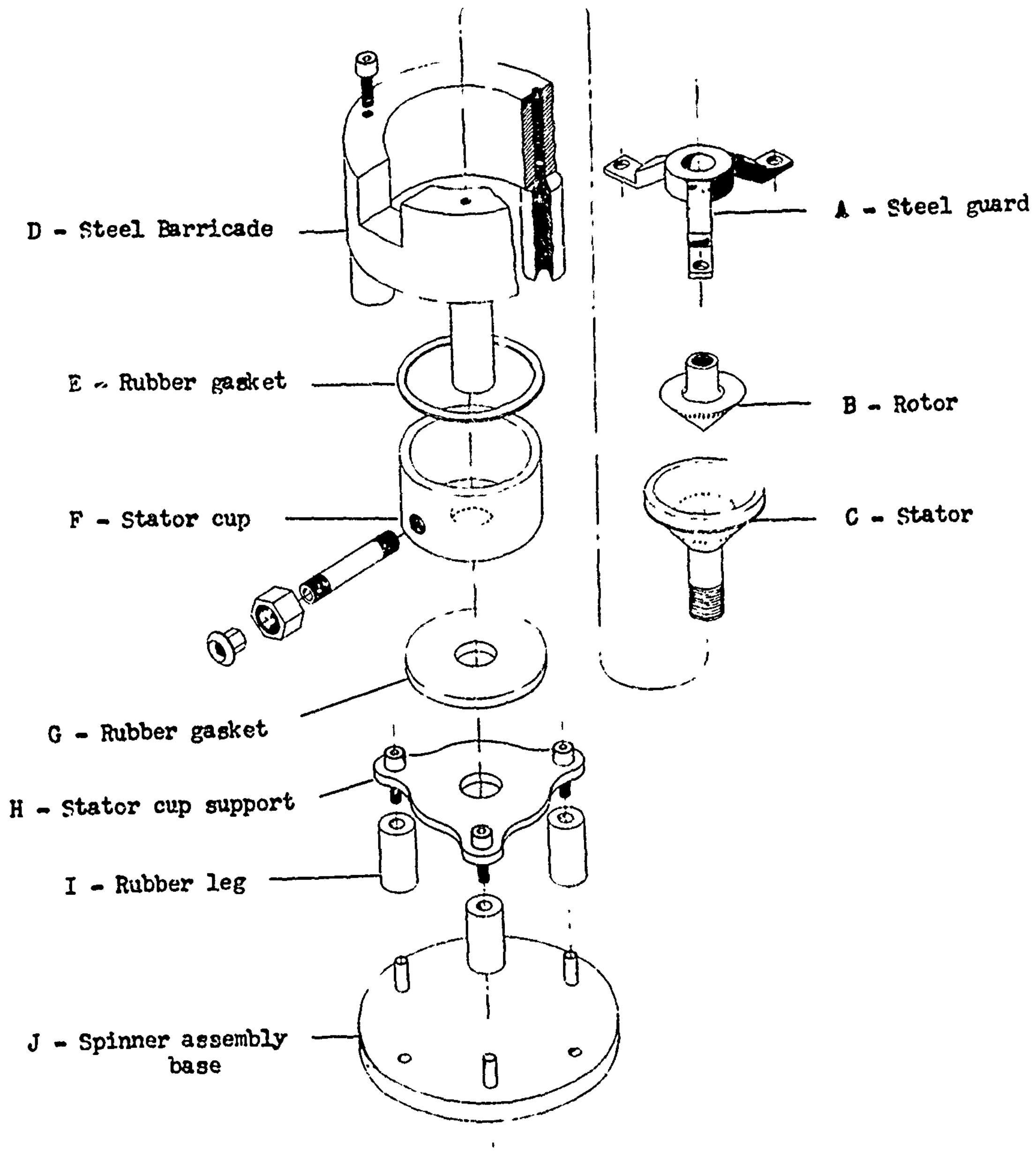

Figure 3. Exploded View of Bullet Spinner Assembly

through a number 60 sieve. The compositions prepared for this study were a stoichiometric blend based on the assumed reaction

$$5\,Mg + Sr(NO_3)_2 \rightarrow 5\,MgO + SrO + N_2$$

and blends containing 30 mole percent more and less magnesium from stoichiometric. These three mixes, which are presented in Table I, were then pressed with a flat punch at 70,000 psi into cold rolled steel capsules 1-1/2" H x 3/4" OD x 3/8" ID. The individually measured column heights were approximately 0.600". A flat punch was used rather than the normal teated punch used in tracer manufacturing in order to provide a flat surface for column length measurements.

TABLE I.

Composition of Binary Fuel/Oxidizer Mixtures

Mixture Description	Weight (%) Mg	$Sr(NO_3)_2$
Stoichiometric	36.3	63.7
Fuel Deficient (-30 mole %)	28.8	71.2
Fuel Rich (+30 mole %)	42.8	57.2

Spin rates used were 0; 20,000; 28,000; 35,000; and 43,000 rpm. Tests at spins between 0 and 20,000 rpm and above 43,000 rpm were not conducted. At the lower values, there was a large variance in speed due to varying air pressure; above 43,000 rpm the spinner became unstable.

Data measurements on the samples included total burning time, candlepower, slag weight retained in the cavity, and spin rate. In order to establish representative candlepower values for the samples tested, the average values for the maxima and minima were taken.

The maxima themselves were not reported because it was believed that they were not representative of the flame phenomenon. For the stoichiometric and the fuel-rich mixtures burned at the higher rotational speeds, candlepower increased as the column burned. For these conditions the maximum representative candlepower value was the one reported.

The amount of slag retained was determined by simply weighing the capsules before and after charging and then again after burning. Weights were obtained only to the nearest decigram because of the handling problems during both the charging and the burning operations.

DISCUSSION

Burning Rate as a Function of Composition and Angular Velocity

The data listed in Table II and plotted in Figure 4 indicate that the average linear burning rate of a $Mg/Sr(NO_3)_2$ binary mixture is directly proportional to the magnesium content of the mixture and also to the rotational speed of the sample. The excess magnesium composition exhibits the highest burning rate at all rotational speeds and the deficient (from stoichiometric) magnesium composition has the lowest burning rate at all rotational speeds, with the stoichiometric mixture always between the two.

It is interesting to note that, for rotational speeds up to and including 43 K rpm and variations of magnesium content of ± 30 mole percent from stoichiometric, the influence of spin on the burning rate can be represented by a simple linear relationship. Using a least squares analysis (Appendix A) on each of the data sets the following three equations were obtained:

For the fuel-rich mixture:

$$r = 0.160 + 1.43 \times 10^{-6} S \quad (1)$$

For the stoichiometric mixture:

$$r = 0.122 + 1.54 \times 10^{-6} S \quad (2)$$

For the fuel-deficient mixture:

$$r = 0.059 + 1.84 \times 10^{-6} S \quad (3)$$

TABLE II.
Burning Rate and Slag Retention Data

A. Burning Rate and Percent Change

Spin Rate (RPM)	Deficient Magnesium: Burning Rate (in/sec)	Deficient Magnesium: % Change*	Stoichiometric: Burning Rate (in/sec)	Stoichiometric: % Change	Excess Magnesium: Burning Rate (in/sec)	Excess Magnesium: % Change*
0	0.059	---	0.120	---	0.160	---
20,000	0.094	59.3	0.159	32.5	0.195	21.8
28,000	0.117	101.8	0.160	33.3	0.195	21.8
35,000	0.118	103.5	0.179	49.1	0.208	30.0
43,000	0.139	135.6	0.186	54.9	0.227	41.9

B. Slag Percent and Percent Change

Spin Rate (RPM)	Deficient Magnesium: Slag Percent	Deficient Magnesium: % Change*	Stoichiometric: Slag Percent	Stoichiometric: % Change*	Excess Magnesium: Slag Percent	Excess Magnesium: % Change*
0	69.5	---	58.3	---	49.1	---
20,000	65.6	-5.6	63.0	8.1	57.4	16.9
28,000	72.4	4.2	64.5	10.6	62.2	26.6
35,000	66.7	-4.1	60.7	4.2	63.7	29.6
43,000	70.0	0.1	66.7	13.1	62.5	27.2

*From static condition

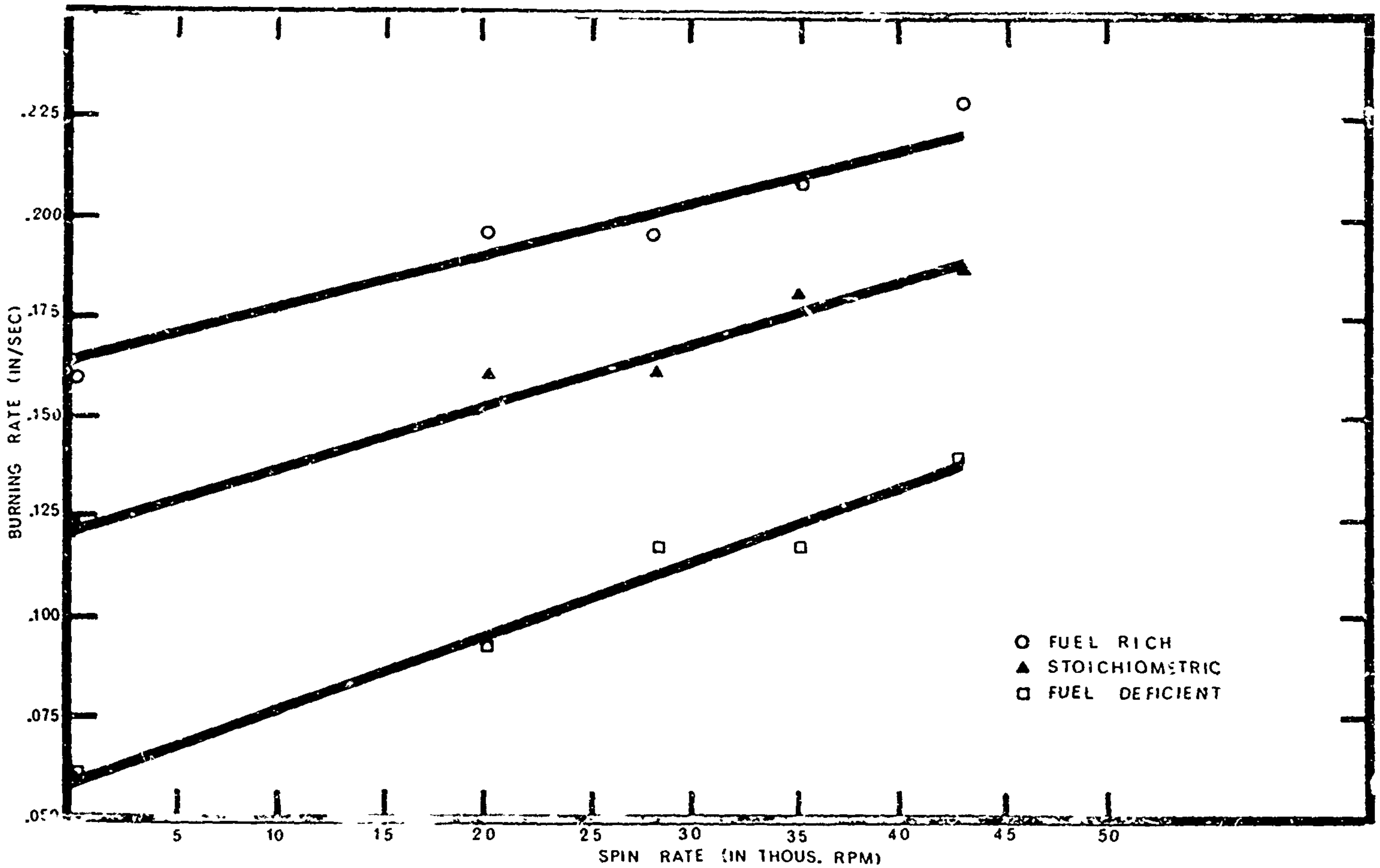

Figure 4. Burning Rate vs Spin Rate for Three Mg-Sr $(NO_3)_2$ Mixes

where r is the average linear burning rate in inches/second, and

S is the spin rate of the sample in revolutions/minute

Taking these three individual equations and applying the appropriate mathematical techniques (Appendix B), a general equation containing both magnesium content and spin rate coefficients results:

$$R = -0.148 + 0.729 \times 10^{-2}(M) - 2.75 \times 10^{-8}(M)(S) + 2.60 \times 10^{-6}(S) \quad (4)$$

where R = linear burning rate in inches/second

M = magnesium percentage

S - spin rate of sample in revolutions minute

This general equation and the experimental data curves are plotted in Figure 5. The parametric equation agrees quite well with the observed data. For example, at the spin/magnesium percentage values of 0/28.8; 43K/42.8; and 28K/36.3; the parametric equation burning rates are 0.062, 0.225, and 0.161 inch/second, respectively. These rates compare favorably to the observed rates of 0.059, 0.227, and 0.160 inch/second, respectively. It was, therefore not deemed necessary to include a scaling factor to have the terminal values correspond with the actual data since this would produce larger percentage errors in the middle of the space.

In the following discussion, References 4, 5, 6, and 7 pertain to the general theories presented on pyrotechnic burning under static conditions, while Reference 8 helped formulate the convex burning

---

[4] A. A. Shidlovsky, "Fundamentals of Pyrotechnics", Picatinny Arsenal Technical Memorandum 1615 (May 1965).

[5] Proceedings Second International Pyrotechnics Seminar, Aspen, Colorada, 20-24 July 1970 (Sponsored by Denver Research Institute, University of Denver), pp 101-115, 269-293.

[6] Proceedings Third International Pyrotechnics Seminar, Colorada Springs, Colorado, 21-25 August 1972 (Sponsored by Denver Research Institute, University of Denver), pp. 435-444, 445-459.

[7] Engineering Design Handbook, Military Pyrotechnic Series, Part One, Theory and Application, AMCP 706-185 (1967).

[8] Private Conversations, Workshop on Basic Processes in Pyrotechnics, NAD Crane, Ind., 11-14 April 1973.

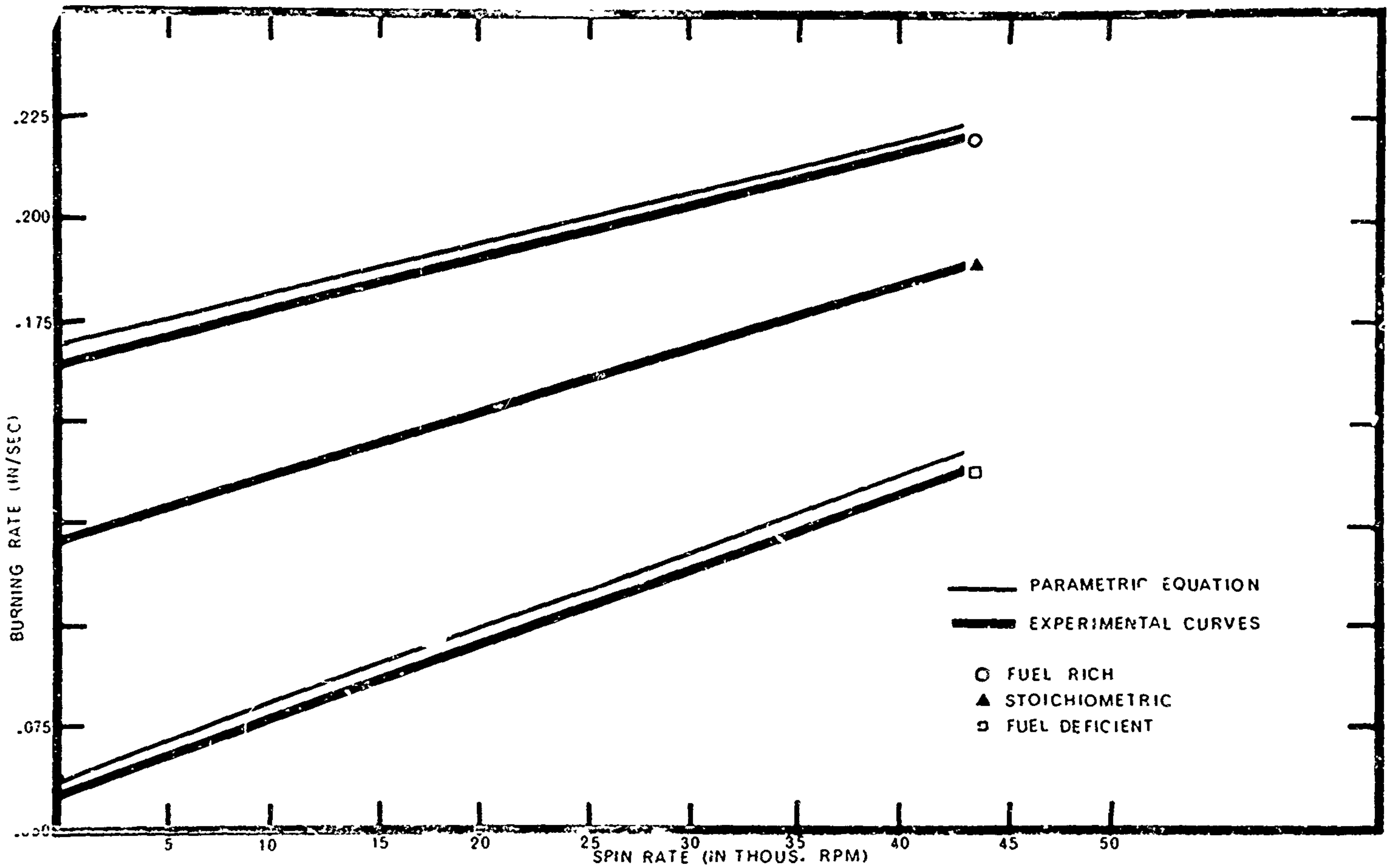

Figure 5 Parametric Equation vs Experimental Curves for Three Mg-Sr $(NO_3)_2$ Mixes

surface model. The discussions on the effects of spin on pyrotechnic burning, however, are the author's.

The combustion of a pyrotechnic is the sum total of many exothermic and endothermic reactions. In discussing the data reported here, a rough division of the actual overall combustion process is made, separating the overall reaction into a condensed or solid-solid/liquid phase and a flame or gaseous phase. In the condensed phase, reactions are endothermic or weakly exothermic and are greatly affected by both outside parameters (compaction pressures, cavity diameter, spin, etc.) and compositional effects (percent ingredients, thermodynamic properties of ingredients, etc.). In the gaseous phase, however, the reactions are highly exothermic and are less affected by outside forces. With this division, the overall reaction process can be effectively analyzed by regarding the condensed phase as the rate determining phase and the flame phase as a heat reservoir for the condensed phase.

In the stoichiometric, static condition, the reaction proceeds at some linear burning rate, R, not affected by the spin variables (S = 0) nor by any excess ingredient variables. This reaction condition produces a laminar burning effect or reaction profile similar to the one outline in the figure below. Region A represents the unreacted portion of the pyrotechnic composition "unaffected" by outside parameters. Region B is the "pre-heated" portion of the curve in which the heat transfer process is noticeable and results in a raising of the composition temperature. Region C is the reaction zone in the condensed

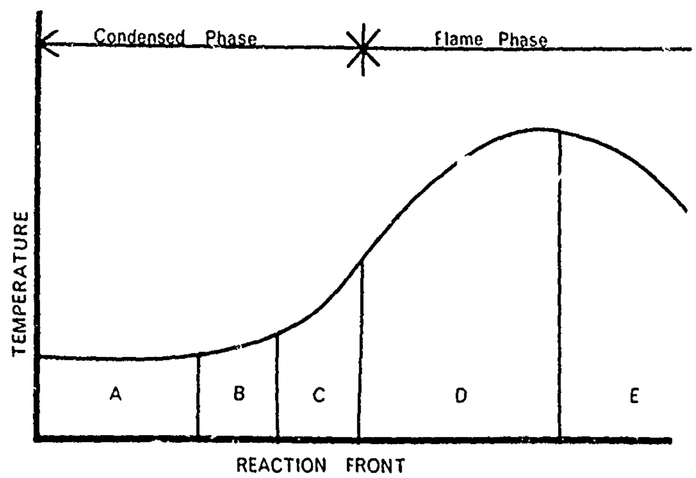

phase. This portion represents the melting and thermal decomposition of the oxidizer and the high absorption of heat from the flame phase. Species exist primarily as liquid and hot solid in this region and are relatively mobile compared to Regions A and B. These three sections together comprise the condensed phase and can be characterized as being generally endothermic and rate-controlling.

The final portion of the reaction profile is the flame phase (D-E). In this phase the temperatures are the highest (D) with reactions primarily being gaseous. In this last stage of combustion, atmospheric oxygen and nitrogen participate in the oxidation. With this addition, the total caloric level of this already exothermic region is enhanced. Subsequently, these flame phase species combine to form stable oxides and these produce the lowered temperature region (E) with final reaction products.

In the fuel-deficient, static condition (as in all other conditions), there is oxidizer which must decompose first to react with the metal to propagate the reaction. With excess oxidizer, however, the preheated region (B) is greatly reduced in temperature due to an abundance of the $Sr(NO_3)_2$ endothermic agent, and the reaction region (C) has a lower temperature. This is due to a shift from the heating of the Mg to the absorption of heat by the $Sr(NO_3)_2$ for decomposition. The excess nitrate decomposition proceeds at a much slower rate and at a higher thermal cost than the magnesium heating process, thus reducing the overall reaction rate. This can be seen from the fact that by reducing the magnesium content 30 mole percent from stoichiometric the reaction rate is lowered 50 percent from 0.120 inch/second to 0.059 inch/second.

In the excess-fuel, static condition, the larger percentage of magnesium acts as an excellent heat conductor. With the moderately high thermal conductivity of magnesium (0.38 cal $sec^{-1}cm^{-1}C^{-1}$ versus 0.18 for iron) the pre-heated region (B) is extended at a higher temperature further into the unburnt column and the composition as a whole absorbs a greater quantity of heat. This results in a lesser amount of additional heat needed to raise the temperature of preheated and combustion zones (B-C) for more rapid decomposition of the nitrate.

The imposition of spin to a binary pyrotechnic column introduces a new parameter in the burning process of the mix. As noted in the data, burning rates increase linearly for each of the mixes up to 43,000 rpm. Also, spin has a greater effect on the mixes with lower percentages of magnesium. This latter fact can be gleaned from the percentage increases in burning rates for each of the mixtures listed in Table II and from the individual slopes of the burning rate Equations 1 to 3.

Spin has different quantitative effects on each of the three mixes but qualitatively the effect is the same. The differences in spin effects primarily result from the compositions themselves and their non-spin burn characteristics. In all cases, the spin effect is most pronounced in the reaction zone of the condensed phase. In this zone, the particle mobility is highest and therefore most susceptible to the radial effects of spin.

Consider the burning pyrotechnic column. A layer of molten reactants exists at the top of the column (region C). This layer is only several mils thick[9], consisting of decomposing $Sr(NO_3)_2$ and high temperature (~450 to 500 C) solid magnesium. With the decomposition of the nitrate, the average molecular weight of this region is considerably lower than the rest of the column. This creates the low density region at the surface of the column to which the addition of spin produces the following:

1. The unburnt portion of the column (A-B) is basically unaffected although the temperature gradient is changed.
2. The flame region (D-E) is moderately affected but less than the condensed phase reaction region. It is noticed that, at the higher spin rates, the plume volume is decreased and the flame is closer to the reaction surface.
3. The condensed phase reaction region particles (C) travel spirally outward, density gradients are formed at and near the surface, heat transfer increases in a radial direction, and the burning surface becomes convex in shape.

---

[9] A. P. Hardt, and P. V. Phung, "Study of Reaction Mechanisms in Tracer Munitions", Final Report Contract Number DAAA25-73-C-0675, March 1974.

For the following discussion, the unburnt portion of the column and the flame phase will not be considered, but only the condensed phase reaction region.

The hot particles at the burning surface are accelerated outward in a spiral-type path. This results in each particle remaining at the surface longer, thus increasing the amount of heat it receives from the flame phase (thus raising its temperature) and also increasing the probability of reaction through both a longer mean path of travel on the reaction surface and a longer time span in which it is in close proximity with other reactants.

While these particles are spinning outward, the tangential component is also forcing these particles to a greater density as the radius increases. Since this layer is molten, the particles on the outward edges of the spinning capsule are closer together, increasing their effective collision frequencies and thus their reaction probability This phenonemon occurs, of course, in a gradient-like increase in the linear burning rates outward resulting in an overall increase in the linear burning rate of the column.

Another effect of spin is the increase in the conductive heat transfer process. This increase is due to the density gradient formed at and near the surface of the column and the fact that the flame is closer to the surface. With the closer flame zone, the heat flux to the column increases. The density gradient of particles then more effectively transfers this heat to the column because of the nearness of the molecules at the higher densities. These two conditions combine to pre-heat the unreacted portion of the sample. As the temperature of the sample is increased, less heat from the flame zone is required for the reactions in the condensed phase. This factor is quantitatively described by the Arrhenius Factor, $e^{-Ea/RT}$. As the temperature increases the negative exponent also increases thus increasing the reaction rate.

The final effect of spin considered in this discussion is the change from a "cigarette-type" burning under static conditions to a convex-type burning while spinning. The convex burning surface is caused by the tangential forces directing the major reaction components towards the circumferential portions of the spinning capsule. Because these effects are increasing with radial distance, the burning rate quite naturally will also increase with radial distance. This produces the convex burning surface sketched in the figure below.

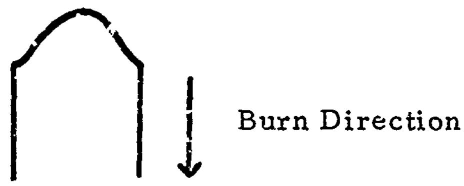

Cross-Sectional View of Burning Pyrotechnic (Spinning)

Recent studies at Frankford Arsenal on the M13 artillery tracer capsule have shown that at 42,000 rpm the burning tracer ejects a pyramidal section of unburnt tracer mixture during the last portion of burning (Figure 8). This expelled section had a base diameter approximately equal to the diameter of the cup with an uncharred portion of the mix at the base of the mix. From this test it appears that with large (.750" diameter) samples, spin does produce the predicted burning surface.

Projecting the above hypotheses to other systems, it would be predicted that for identical mixes at identical spin rates, a capsule with a larger internal diameter would have a higher burning rate than those with smaller diameters, since the tangential forces would increase as one proceeds radially from the center. Figures 6 and 7 (2) are presented to support this theory. It is noticed that in all cases the greater the diameter of the capsule the greater the burning rate (shorter burning time). The difference in the shapes of the curves is probably due to compositional effects of the multi-component mixtures.

Candlepower as a Function of Composition and Angular Velocity

The light outputs of the pyrotechnic samples are presented in Table III and Figure 9. From these, the general relationships between magnesium content, spin and candlepower can be seen. As magnesium content is increased the flame intensity also increases.

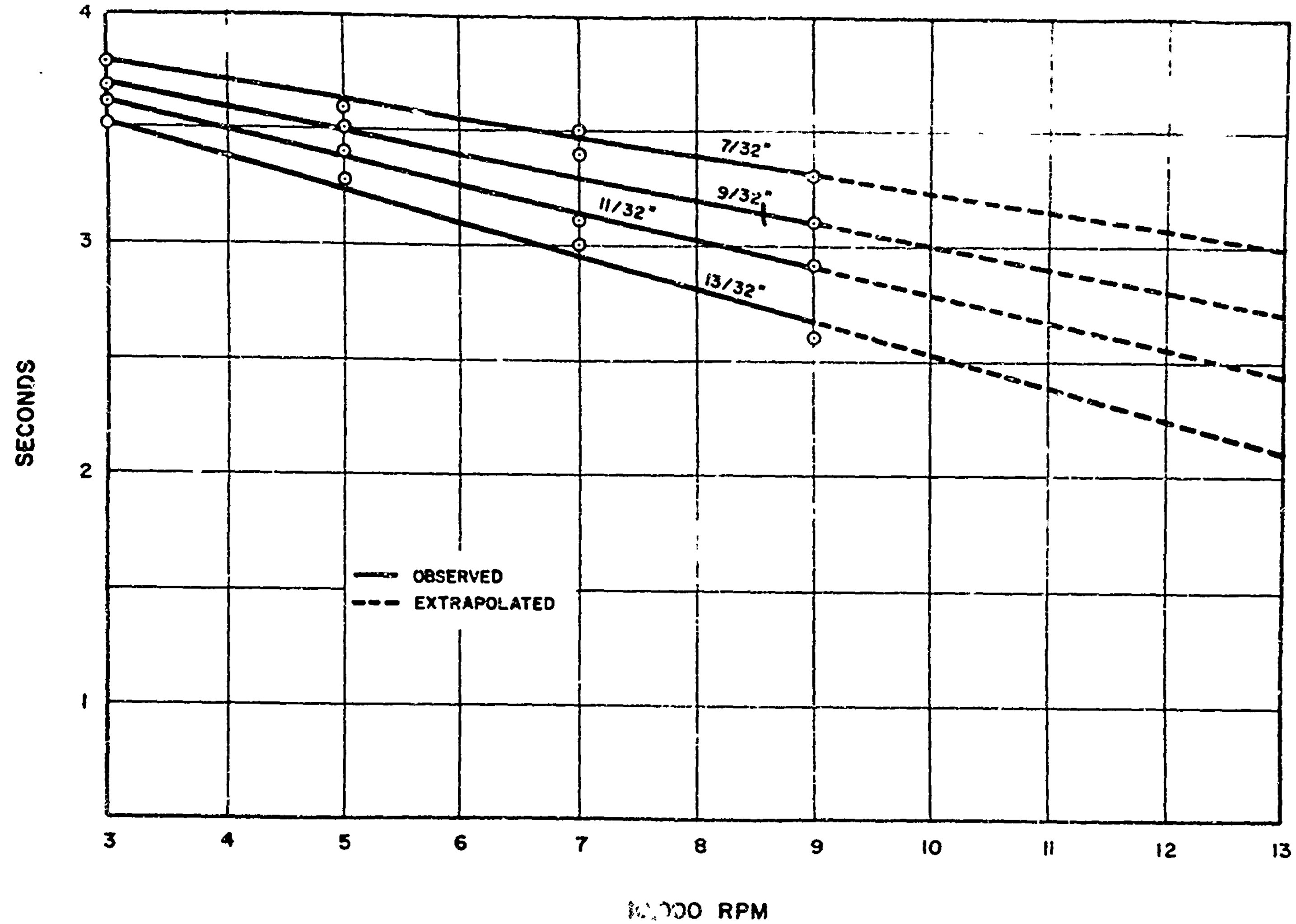

Figure 6. Effect of Spin Upon Trace Duration of Tracer Composition R-256 Charged in Various Diameters in a 9/16 Inch Column

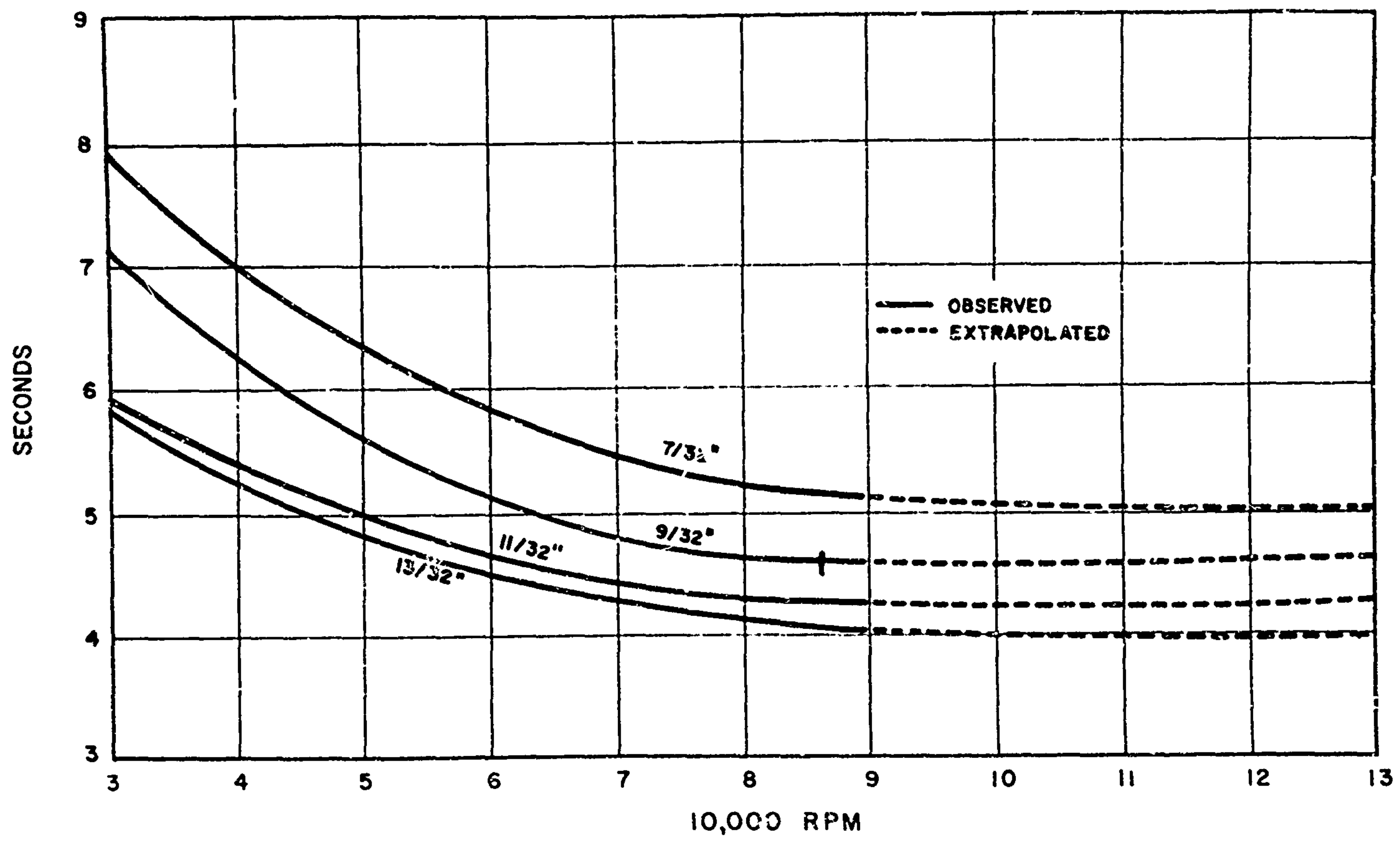

Figure 7. Effect of Spin Upon Trace Duration of Tracer Composition R-257 Charged in a 9/16 Inch Column of Various Diameters

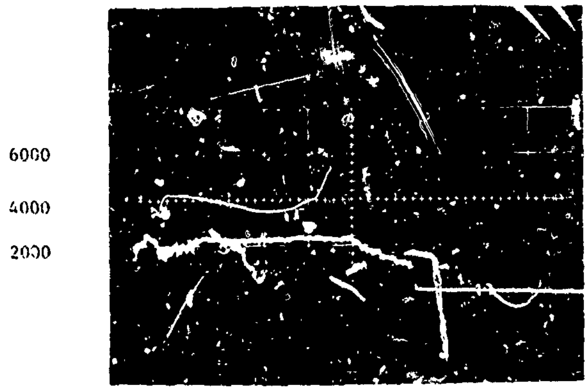

TIME (.5 SEC/CM) VS CANDLEPOWER (2000 [illegible]

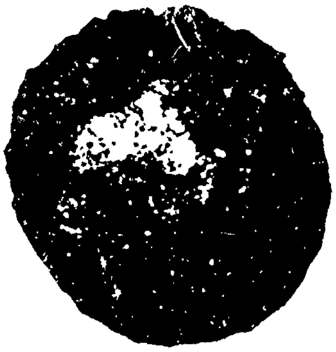

Figure 8. Burning Time, Luminosity, and Ejected "Cone" Photographs (10X) of M13 Artillery Tracer Spin at 42,000 rpm

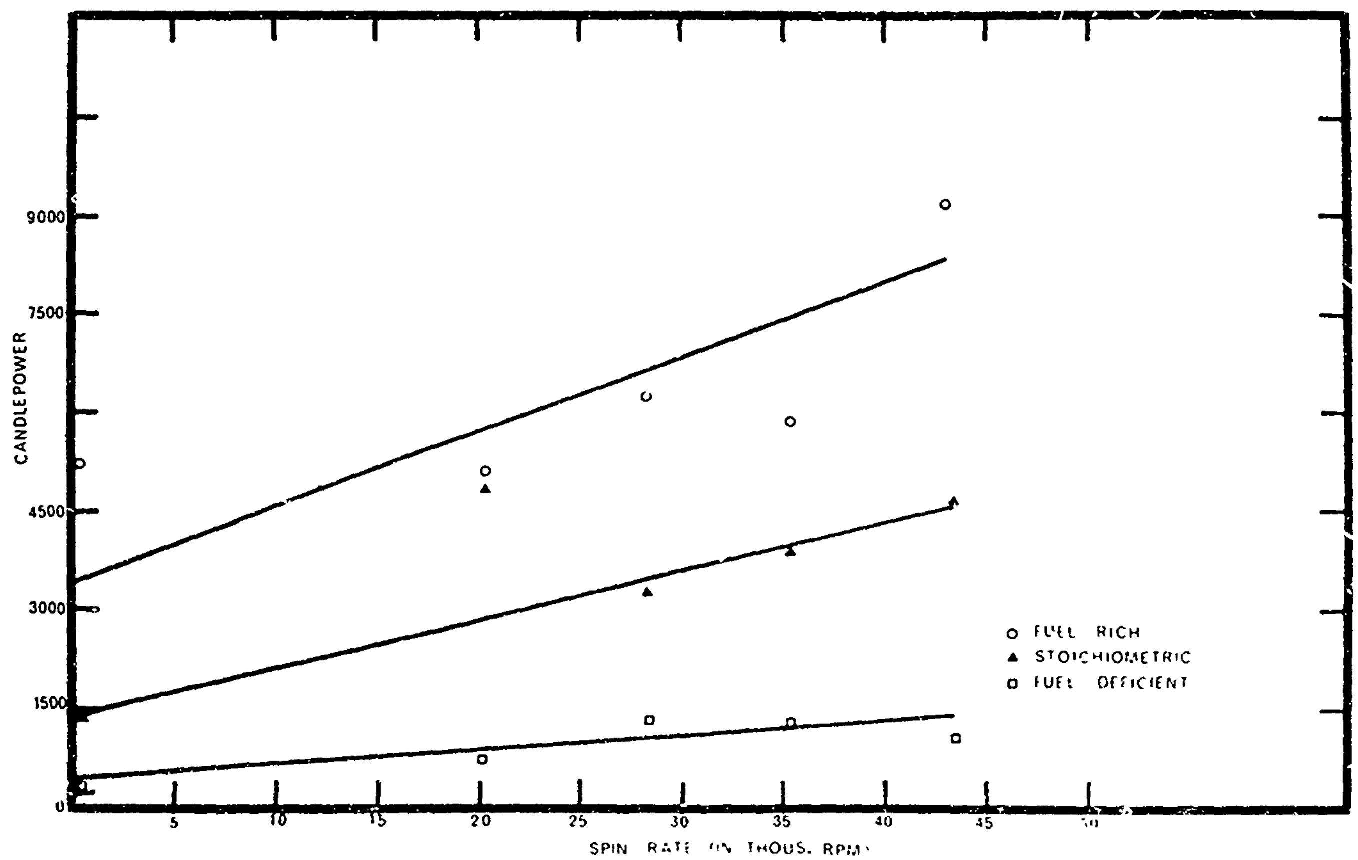

Figure 9. Candlepower vs Spin Rate for Three Mg-Sr $(NO_3)_2$ Mixes

TABLE III.

Candlepower vs Spin Rate for Sample Mixes

Spin Rate (rpm)	Maximum Candlepower		
	Deficient Magnesium	Stoichiometric	Excess Magnesium
0	180	1400	5100
20,000	700	4600	4800
28,000	1350	3200	6200
35,000	1250	3750	5750
43,000	950	4550	9050

As spin is introduced the data indicate that the higher the magnesium content the greater the increase in luminosity. Figure 9 shows this general trend.

For the deficient magnesium sample, spin has little effect on light output. This is probably due to the lack of sufficient thermal energy to raise the magnesium to a level of high emission. Most of the heat of reaction is absorbed by the excess $Sr(NO_3)_2$ for decomposition. This produces magnesium particles to be ejected at a much lower temperature and therefore a lower luminosity.

The stoichiometric mixture has the highest adiabatic flame temperature. This results in the highest intrinsic thermal radiation of the three mixes studied. (As the temperature is raised the amount of energy emitted by the flame is increased by a power of four according to the Stefan-Boltzman Law.) Even though the flame is not a black body, one can see that even a first approximation would give a considerable quantity of light.

At approximately 500 C, luminescence begins to appear due to the atoms and ions in the flame being excited to higher energy levels and then emitting visible light as they return to the ground state. Since pyrotechnic flames are at least five times hotter than this minimum temperature requirement, luminescence can be considered an integral part of flame phenomenon. Therefore, with the addition of luminescence to the already greatly increased thermal radiation of the hotter stoichiometric flame, this mixture will emit more strongly than the fuel deficient mixture.

The fuel-rich mixture has the highest <u>total</u> light output. Its flame temperature is lower than the stoichiometric mix; but, with the excess magnesium reacting with atmospheric oxygen on the outer edges of the flame the overall light output is greater than either of the two other mixes. Also, since there are additional reactions occurring at the edges of the flame, the plume of the fuel-rich mixture is larger than the others. This factor causes an increase in total flame volume which in turn increases the total light output.

Figures 10 and 11 present candlepower versus burning time for the three mixes in static and spin conditions, respectively.

In Figure 10, erratic burning conditions are more pronounced as magnesium content increases. This erratic burning is related to the increased burning rate and the greater thermal diffusivity of higher magnesium content mixes. As the magnesium content increases, the rate of decomposition of the nitrate in the condensed phase increases which in turn causes larger particles of fuel and oxidizer to be ejected With these ejected fragments, a portion of the heat from the reaction is lost which causes a reduction in the heat flux to the preheated regions and, therefore, a reduction in the overall reaction and light output. As more mixture is decomposed on the surface and heat is again being released in large quantities, the reaction increases to the point where another "large chunk" of mix is ejected. This pulsating-type reaction is less noticeable at lower percentages of magnesium because there is less pre-heating at the lower percentages.

Figure 11 demonstrates the effect of spin on light output. At 43,000 rpm, as the magnesium content increases (accelerating the burning process), both the total light output and the change in light output versus burning time increases (Figure 10). This increase in luminosity is probably due to the same basic reactions occurring in a shorter period of time. This produces the same amount of light energy in less time resulting in an increase in luminosity. Also, as the sample spins, greater surface area is created due to the convex burning surface. This could contribute significantly to the differences in light output since the faster the spin, the faster the reaction and the greater the convex surface. As the surface of an emitter increases, the greater is the luminous flux.

Slag as a Function of Composition and Angular Velocity

The slag percentages of the mixes studied appeared to be inversely related to magnesium content at static burn but have no direct relationships to either magnesium content or spin rate above 30,000 rpm (Table II, Figure 12). An explanation of this phenomenon is apparent from Figures 10 and 11.

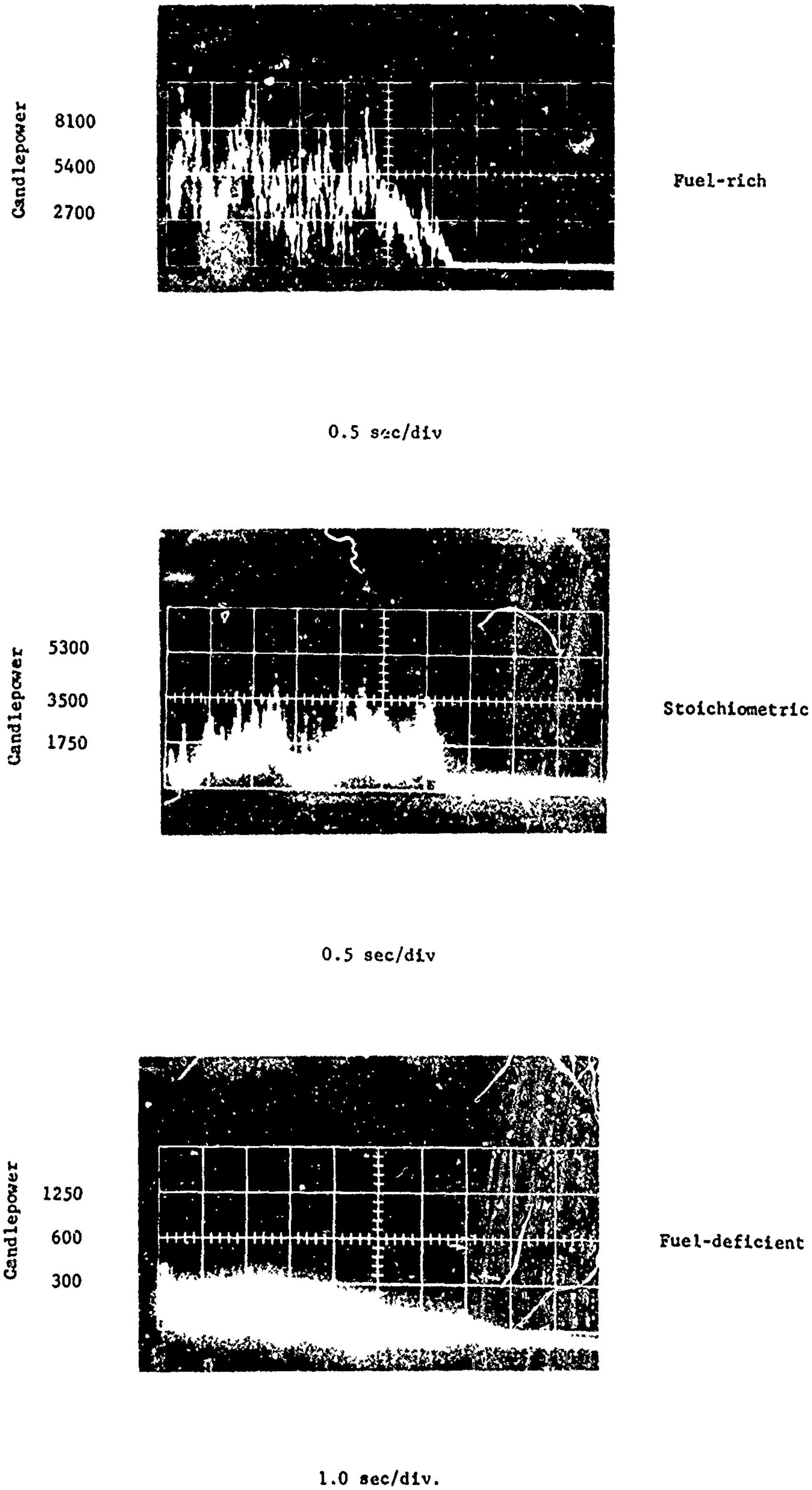

Figure 10. Sample Oscillograms of Candlepower vs Burning Time for Static Conditions

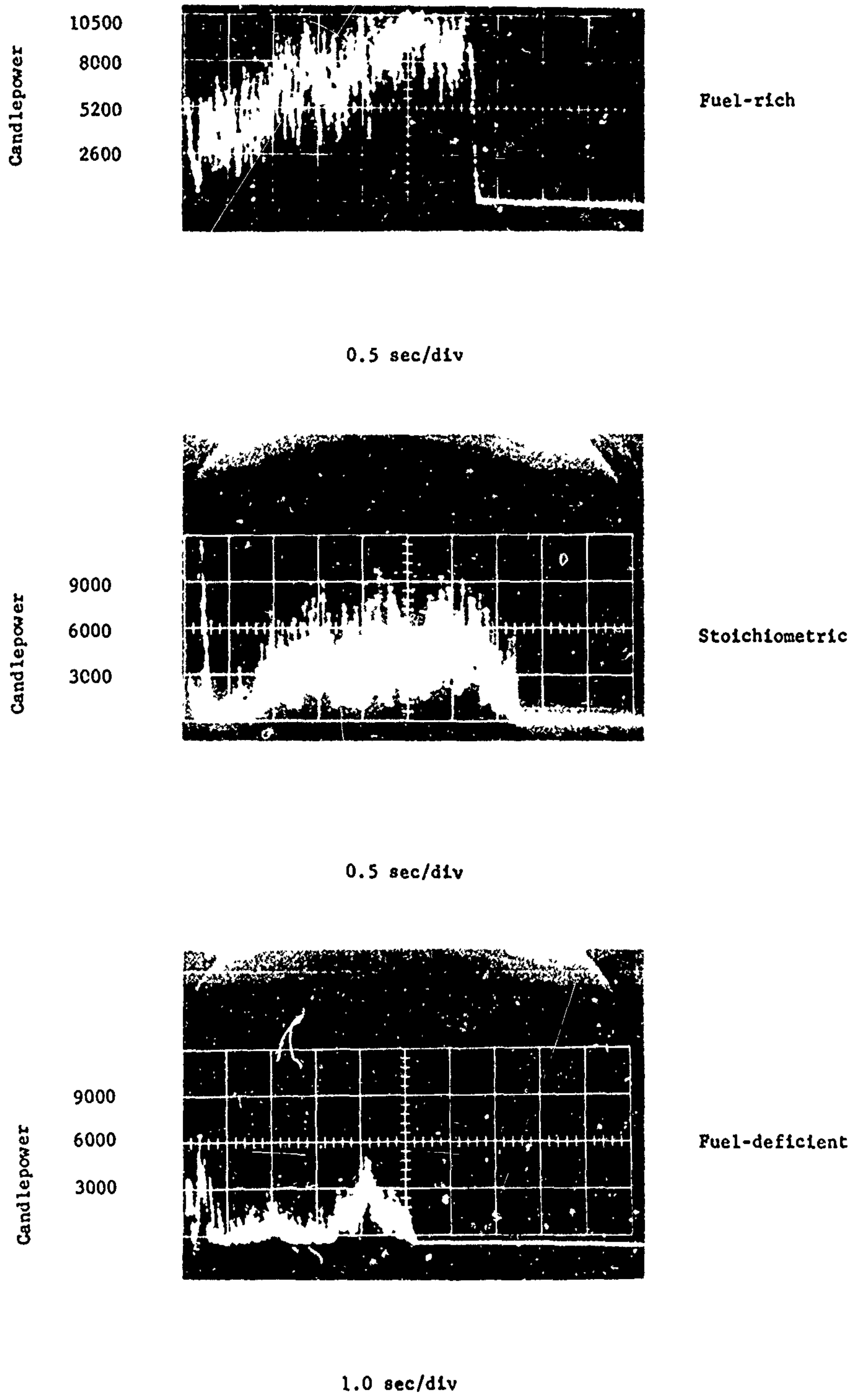

Figure 11. Sample Oscillograms of Candlepower vs Burning Time for 43,000 rpm Condition

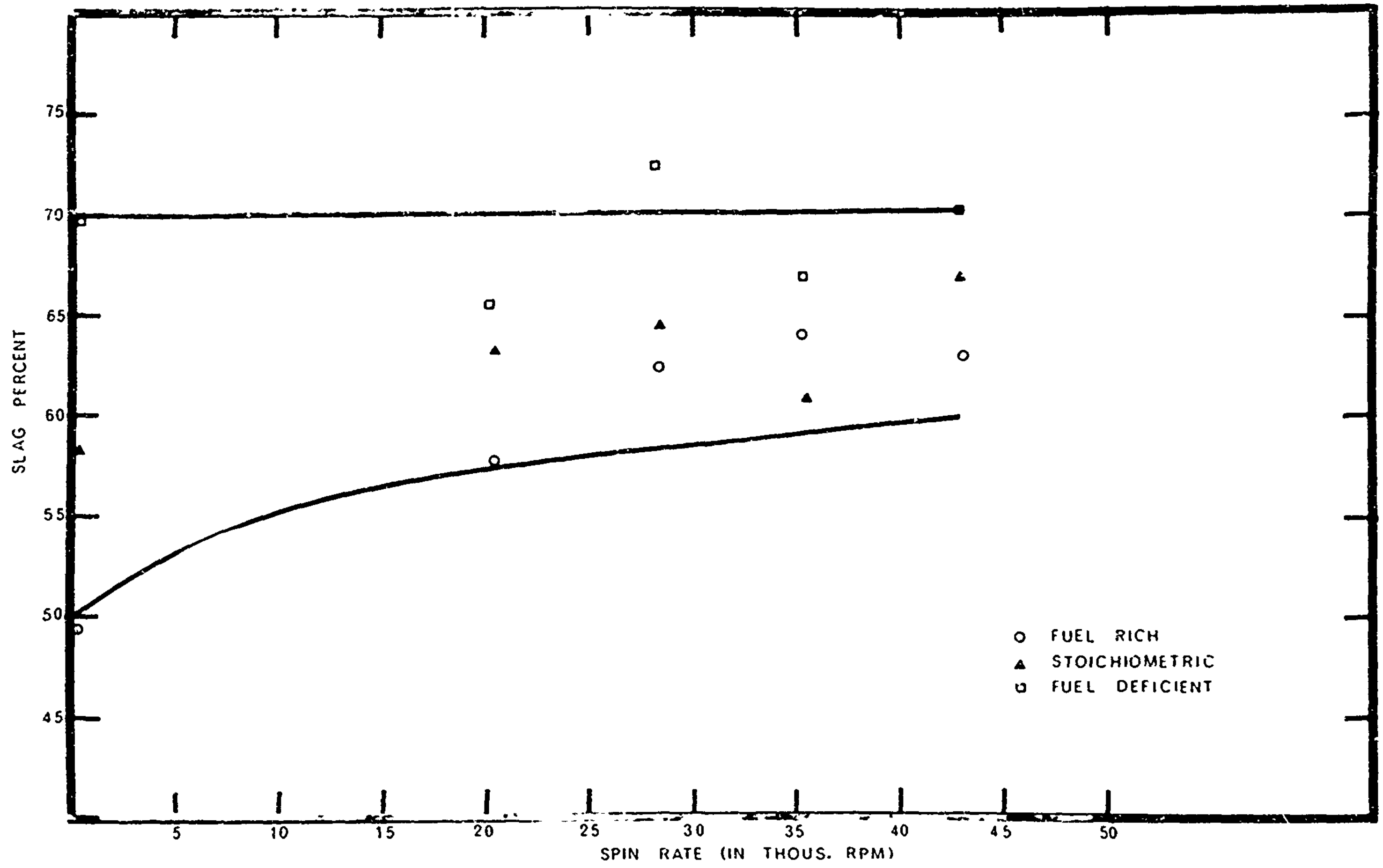

Figure 12. Slag Percent vs Spin Rate for Three Mg-Sr $(NO_3)_2$ Mixes

With increased magnesium content, the light output at static burn becomes more irregular due to the expulsion of larger particles of unburnt mix (Figure 10). Also, since more mix is being expelled, there is less slag retained (the percentage slag of the fuel-deficient mixture was 69.5 percent, while the excess-fuel mixture had a slag percentage of 49.1 percent).

As the sample is spun (Figure 11), the particles are held in the capsule for a longer period of time during reaction and therefore less variation in light output occurs with fewer large particles being ejected. The percent slag of the three mixes tends toward a mean value of 65 percent because at the higher spin rates there is not enough energy from the reactions to force their proportionate residues from the capsule. The radial forces of the spinning capsule exert an increasingly greater force parallel to the surface of the burning mix than the force exerted normal to the surface generated by the reaction For this reason, all three samples will have approximately the same percentage of high density reacted material along the inside edge of the capsule wall.

CONCLUSIONS

1. The burning rate of a $Mg/Sr(NO_3)_2$ mixture consolidated at 70,000 psi into a 0.375" ID cylindrical cavity is given by the equation:

$$R = -0.148 + 0.729 \times 10^{-2}(M) - 2.75 \times 10^{-8}(M)(S) + 2.60 \times 10^{-6}(S)$$

where

R = burning rate in inches/seconds

M = magnesium percentage between 28.2 and 42.8

S = spin rate of sample in rpm up to 43,000

2. The linear burning rate of a pyrotechnic increases as the tangential moment of the sample increases. The greater the spin rate of the sample or the greater the cavity diameter at the same spin rate, the faster the burning rate.

3. Luminosity increases with increasing magnesium content and increasing spin rate of the sample.

4. Slag percent is unaffected at high spin rates (> 30,000 rpm) and appears not directly related to the magnesium content of the mixture at these higher rates.

5. The burning surface of a spinning pyrotechnic becomes convex due to the tangential forces directing the major reaction components towards the circumference of the spinning capsule.

RECOMMENDATIONS

1. This work should be expanded to study the phenomena of burning rate, slag percent, and luminosity at spin rates greater than 43,000 rpm and as a function of cavity diameter.

2. A thermodynamic analysis should be initiated to produce data on pyrotechnic burning to substantiate the theories promulgated in this report.

3. Spectral analysis of the flame should be undertaken to determine the actual reactions and where they occur in the flame zone to better predict the heat flux to the surface.

APPENDIX A

Method of Least Squares*

The problem is to find the burning rate equation for a particular magnesium content mixture which best fits the experimental data points:

r (burning rate)	r_1	r_2	r_3	r_4	r_5
s (spin in rpm)	0	20K	28K	35K	43K

The equation of the line is assumed to be:

$$r = r_o + a(s) \tag{A-1}$$

where: r = observed burning rate

r_o = "true" burning rate at 0 rpm (ordinate intercept)

a = constant (slope of the equation)

s = spin rate of sample (in rpm)

Substituting each data pair into Equation (A-1) generates the following five equations:

$$r_1 = r_o \tag{A-2}$$

$$r_2 = r_o + a(20K) \tag{A-3}$$

$$r_3 = r_o + a(28K) \tag{A-4}$$

$$r_4 = r_o + a(35K) \tag{A-5}$$

$$r_5 = r_o + a(43K) \tag{A-6}$$

* For a complete mathematical treatise the reader is directed to any advanced calculus or analytical geometry text.

Multiplying each individual equation by the coefficient of r_o of that equation (in this case 1) and summing the five equations yields:

$$\sum_{i=1}^{i=5} r_i = 5\,r_o + 126\,K(a) \tag{A-7}$$

Multiplying each equation by the coefficient of (a) of that equation, namely by (s), and summing the five equations yields:

$$\sum_{i=1}^{i=5} s_i\,n_i = 126\,r_o + 4258\,(a) \tag{A-8}$$

Equations (A-7) and (A-8) may now be solved simultaneously to produce r_o and a for Equation (A-1).

APPENDIX B

Construction of a Parametric Equation

Data is presented which equates burning rate, (R), with spin (S), and burning rate with magnesium content (M). The task is now to derive an equation which correlates spin and magnesium content to the burning rate. Mathematically, the problem is to find the equation:

$$dR = \left(\frac{\partial R}{\partial M}\right)_S dM + \left(\frac{\partial R}{\partial S}\right)_M dS \qquad \text{(B-1)}$$

To solve for the first term of the differential, plot the burning rate at zero spin versus percent magnesium. The three data pairs used for this plotting come from the least squares analysis of the experimental data:

$$R_1 = 0.160 + 1.43 \times 10^{-6} \text{ (S)} \qquad \text{(B-2)}$$

$$R_2 = 0.122 + 1.54 \times 10^{-6} \text{ (S)} \qquad \text{(B-3)}$$

$$R_3 = 0.059 + 1.84 \times 10^{-6} \text{ (S)} \qquad \text{(B-4)}$$

results in a general equation to describe the change of burning rate, R, with change in magnesium content, M, at zero spin:

$$R_M = 0.148 + 0.729 \times 10^{-2} \text{ (M)} \qquad \text{(B-5)}$$

Plotting slopes of the three equations (B-2, B-3, B-4) versus magnesium content and finding the best-fit equation yields:

$$R_S = 2.60 \times 10^{-6} - 2.75 \times 10^{-8} \text{ (M)} \qquad \text{(B-6)}$$

The above equation gives the change in the burning rate versus spin for a composition having a magnesium content equal to M.

Combining Equations (B-5) and (B-6) yields a generalized equation to determine burning rate at spin, S, and magnesium content, M.

$$R = R_M + R_S (S) \tag{B-7}$$

Substituting the expressions for R_M and R_S (Equations B-5 and B-6) into Equation B-7 yields:

$$R = -0.148 + 0.729 \times 10^{-2}(M) + \left\{2.60 \times 10^{-6} - 2.75 \times 10^{-8}(M)\right\}(S) \tag{B-8}$$

By rearranging Equation B-8, the following is immediately obtained:

$$R = -0.148 + 0.729 \times 10^{2}(M) - 2.75 \times 10^{-8}(M)(S) + 2.60 \times 10^{-6}(S) \tag{B-9}$$

REFERENCES

1. R. Shulman, "Factors Affecting Small Arms Tracer Burning", Frankford Arsenal Technical Report R-1287 (September 1955).

2. R. Shulman, "Effect of Cavity Geometry Upon Small Arms Tracer Burning", Frankford Arsenal Technical Report R-1421 (November 1957).

3. J.W. Beams, E.G. Pickels, "The Production of High Rotational Speeds", Rev. Sci. Inst. 6, (1935).

4. A.A. Shidlovsky, "Fundamentals of Pyrotechnics", Picatinny Arsenal Technical Memorandum 1615 (May 1965).

5. Proceedings Second International Pyrotechnics Seminar, Aspen, Colorado, 20-24 July 1970 (Sponsored by Denver Research Institute, University of Denver), pp. 101-115, 269-293.

6. Proceedings Third International Pyrotechnics Seminar, Colorado Springs, Colorado, 21-25 August 1972 (Sponsored by Denver Research Institute, University of Denver), pp. 430-444, 445-459.

7. Engineering Design Handbook, Military Pyrotechnic Series, Part One, Theory and Application, AMCP 706-185 (1967).

8. Private Conversations, Workshop on Basic Processes in Pyrotechnics, NAD Crane, Ind., 11-14 April 1973.

9. A.P. Hardt, and P.V. Phung, "Study of Reaction Mechanisms in Tracer Munitions", Final Report Contract Number DAAA25-73-C-0675, March 1974.